Pergamon

Cement and Concrete Research, Vol. 28, No. 3, pp. 365–379, 1998

0008-8846/98 $19.00 + .00

PII S0008-8846(98)00259-7

MODELING THE DYNAMIC CORROSION PROCESS IN CHLORIDE CONTAMINATED CONCRETE STRUCTURES

T. Liu and R.W. Weyers[1]
Charles E. Via Department of Civil Engineering, Virginia Polytechnic Institute and State University, Blacksburg, VA 24061 USA

(Received December 20, 1996; in final form November 19, 1997)

ABSTRACT

Corrosion of steel in concrete under service conditions is a process strongly influenced by the dynamics of environmental exposure. A total of 44 simulated bridge deck slabs were cast, and corrosion parameters were measured over a 5-year period. The monitored parameters included corrosion rate (linear polarization technique with and without a guard ring) and the concrete ohmic resistance and temperature. A series of 7 corrosion rates were established by admixing increasing amounts of sodium chloride. A non-linear regression model was developed, which demonstrates that corrosion of steel in concrete in service exposure conditions is a function of the concrete chloride content, temperature and ohmic resistance, and active corrosion time. Corrosion weight loss measurements demonstrated that the average annual corrosion rate is better estimated by the unguarded linear polarization method rather than the guarded ring method. © *1998 Elsevier Science Ltd*

PAPERS

Introduction

Chloride-induced corrosion of steel in reinforced concrete structures is one of the major causes of the deterioration of today's infrastructure. The corrosion process of steel in reinforced concrete is generally considered an electrochemical process (1–3). However, electrochemical corrosion of steel in concrete has a number of process characteristics that are determined by the peculiarities of electrochemical reactions in the complex "concrete electrolyte." These characteristics are strongly affected by the heterogeneous structure of the concrete and the structures' environmental exposure conditions.

Corrosion rate is an important parameter for quantitatively predicting the service life of reinforced concrete structures limited by corrosion deterioration (4–6). Current linear polarization technology such as the 3LP and Gecor devices have successfully been used for measuring the corrosion rate (corrosion current density) in reinforced concrete structures (7–8). But the measured corrosion rate from these devices is only an instantaneous value corresponding to a certain concrete temperature and moisture content at the measurement moment. Because of the dynamic nature of concrete and environmental exposure conditions,

[1]To whom correspondence should be addressed.

TABLE 1
Experimental design.

Chloride series, kg/m^3	0.00	0.36	0.71	1.42	2.85	5.69	7.20
Cover depth, mm							
25							4
51	2	3	9	3	3	3	
76	2	3	3	3	3	3	

the corrosion of steel in concrete is highly dependent on many factors such as the concrete temperature, moisture content, ohmic resistivity and salt content, and the supply of oxygen to the cathode site. These factors simultaneously influence the corrosion process and cannot be separated or isolated from each other. Most research work in accelerated corrosion tests is limited to the effects of an individual factor that affects the corrosion process (9–12). The interaction model for characterizing the corrosion rate has not been sufficiently studied because of the complexities of the corrosion process in concrete and the lack of long-term field corrosion data. Thus, it is necessary to develop an interaction model to characterize the corrosion rate, which can then be adjusted to an equivalent value according to the structures' exposure conditions. Thus, the service life of reinforced concrete structures can be better predicted for different environmental exposure conditions. This paper presents an examination of significant factors affecting the corrosion process and an interaction model for characterizing and predicting the corrosion rate based on a 5-year corrosion study obtained from a partial factorial experimental design that simulates reinforced concrete bridge decks.

Experimental

Table 1 presents the partial factorial experiment, with 7 different corrosion rates (different amount of chloride mixed in the fresh concrete), 2 concrete cover depths, reinforcing steel sizes, and spacing. A total of 40 outdoor exposure specimens were constructed in August, 1991. The four specimens with 25 mm cover depths were constructed in late June, 1995. All the specimens shown in Table 1 were constructed with 16 mm diameter bar and 203 mm bar spacing except for the 0.71 chloride—51 mm cover depth cell, which had an additional 3 specimens with 16 mm diameter bar and 152 mm spacing and 3 specimens with 19 mm diameter bar and 203 mm spacing. Concrete specimens 1180 $\times$ 1180 $\times$ 216 mm, simulating concrete bridge slabs, were constructed with 5 electrical isolated reinforcing steel bars (see Fig. 1). Type T thermocouples were placed at the depth of steel surface and used to determine the internal temperature of the steel/concrete interface at each measurement moment. The concrete mixture properties are presented in Table 2.

The 3LP and Gecor devices were used to measure the corrosion current density. Both devices use the same linear polarization technique. A brief description of the two devices follows.

The 3LP is a potentiostatic test with a rectangular counter electrode of 76 mm $\times$ 178 mm. A copper-copper sulfate half cell is used to monitor the change in potential of 4, 8, and 12 mV while measuring the resulting current. The polarization rate is operator controlled within 1.5 to 2.5 min. in approximately 3 equal parts for 0 to 4, 4–8, and 8–12 mV. Within 2 min. after the current is returned to zero, the voltmeter reading should be within 2.0 mV of the

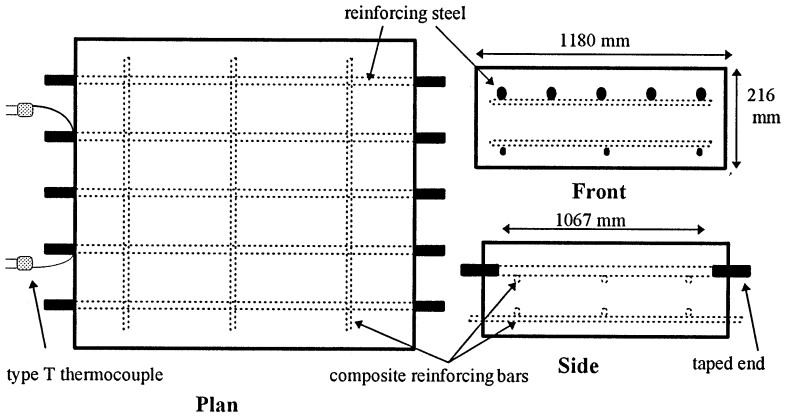

FIG. 1.
A schematic diagram of the slab design.

static potential for the test to be valid. A linear regression analysis is conducted to determine the slope of the current-potential curve (cathodic polarization curve) and a Tafel slope constant of 40 mV/decade is used in the Stern-Geary equation to calculate the corrosion rate. The assumed polarization area is the surface area of the measured reinforcing bar over the length of the counter electrode, 178 mm. The resistance of the cover concrete is removed by the devices' electronic circuitry during the measurement of the slope of the cathodic polarization curve.

The Gecor device uses the galvanostatic method to measure the corrosion rate; the polarization current is controlled and the resulting change in potential is measured. The measurement probe used in this study had an 80 mm diameter counter electrode, a 50 mm wide annular space between the counter electrode and the guard ring, and a 30 mm wide annular guard electrode. Three silver-silver chloride half cells were mounted on the probe, one in the center of the probe-counter electrode and two in the annular space between the counter electrode and the guard ring, one 55 mm and one 75 mm along a radial line from the center of the probe-counter electrode. The polarized area of the working electrode (reinforcing bar) is said to be the surface area of the bar over a length midway between the outer two half cells, or 130 mm in length. The device controls the rate of polarization based on its estimate of the rate of corrosion of the working electrode, and controls the guard ring confining current by monitoring the difference between the outer two half cells. The device measures the resistance of the cover concrete, and subtracts it from the measured polarization resistance to determine the polarization resistance of the working electrode. In addition to

TABLE 2
Concrete mixture properties.

Chloride series, kg/m^3	0.0	0.36	0.71	1.42	2.85	5.69	7.20
Cement, kg/m^3	381	381	379	379	379	337	382
w/c ratio	0.45	0.42	0.42	0.41	0.44	0.43	0.45
Slump, mm	150	100	170	80	100	100	125
Air content, %	3.2	5.0	5.4	4.2	4.7	6.7	5.9
Str. @28d, MPa	30.9	39.1	34.9	39.6	35.9	31.9	35.6

TABLE 3
3LP and Gecor guidelines.

I_{CORR} ($\mu A/cm^2$)	Gecor device corrosion state	I_{CORR} (mA/ft^2)	3LP device expectation
<0.1	Passive	<0.2	No damage expected
0.1–0.5	Low corrosion	0.2–1.0	Damage possible 10–15 years
0.5–1.0	Moderate	1.0–10.0	Damage possible 2–10 years
>1.0	High corrosion	>10.0	Damage possible <2 years

Note: 1 mA/ft^2 = 1.08 $\mu A/cm^2$.

controlling the polarization rate and confining current, the device's computer calculates the corrosion rate using a Tafel slope constant of 26 mV/decade. Typical measurement times are 2 to 5 min.

The result of the differences between the two instruments is approximately an order of magnitude difference in the measured corrosion current density. The general guidelines for interpreting the results of the 3LP (13) and Gecor (14) supplied by the instrument manufacturers are summarized in Table 3.

The monthly corrosion data consist of corrosion rate, corrosion potential, ohmic resistance of the concrete, and the temperature of the concrete for each measurement time. Metal loss measurements were performed in accordance with ASTM G1–90, Method C3.5, and compared with the measured corrosion rates for specimens that cracked.

Results

Measured Corrosion Parameters

Figures 2 to 5 present the measured corrosion rates (3LP and Gecor), cover concrete ohmic resistance, and temperature for 4 of the 7 admixed chloride series in outdoor specimens with 51 mm cover depth as a function of time. As shown, the corrosion rate measurements, both the 3LP and Gecor, are strongly affected by the temperature and ohmic resistance of the concrete. The dynamic corrosion process is related to the changes in the concrete temperature and moisture content. However, the concrete moisture content is influenced by the interactions of time, temperature, and precipitation. Among the admixed chlorides series, the measured corrosion rates increase as the chloride content increases. For the low admixed chlorides series 0.71 kg/m^3 and lower, it is noted that the measured corrosion rates are relatively high during the early time periods and after about 2 years decrease to a low near-constant rate. This is related to the gradual formation of the passive film on the steel surface. For the high admixed chlorides series 1.42 kg/m^3 and higher, the passive film is not easy developed and corrosion takes place continuously; the higher measured corrosion rates are also observed in the early stage, which may be related to the change of area ratio of anode and cathode and an increase in the thickness of the corrosion layer. It is also observed that the ohmic resistance of concrete decreases as the admixed chloride content increases; this is due to the increase of ionic conductivity of concrete as the salt content increases in the pore water of concrete.

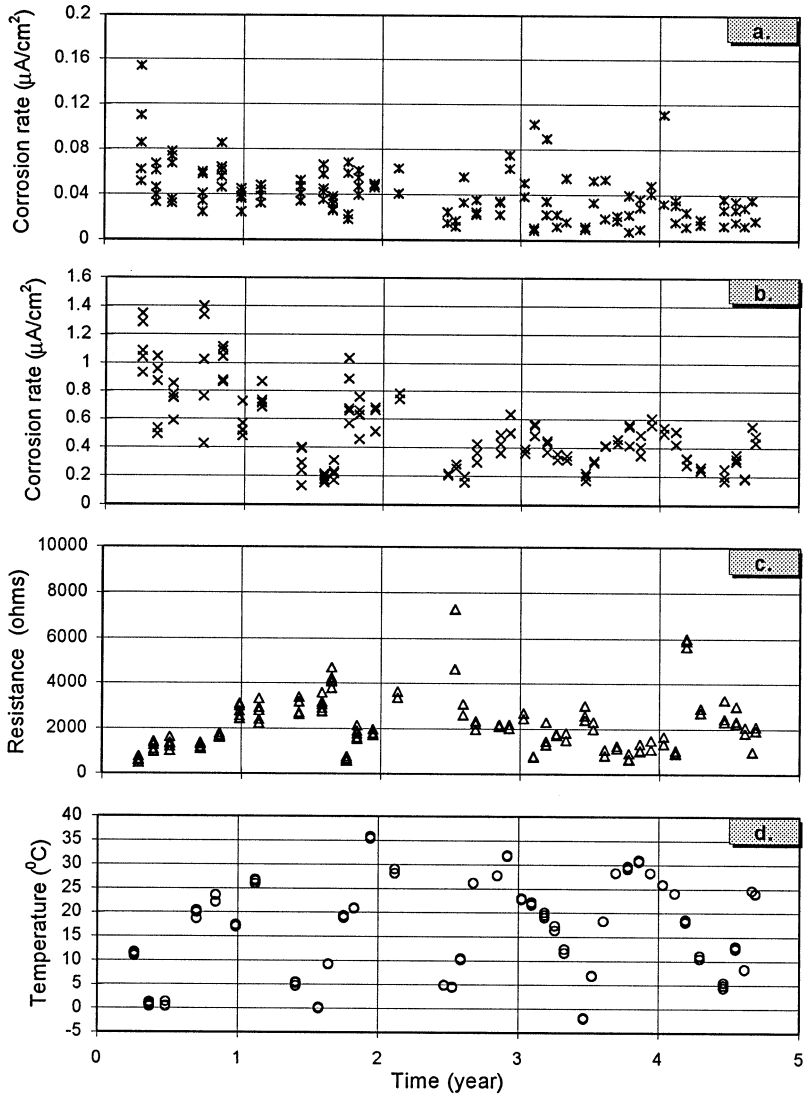

FIG. 2.

Corrosion rate, concrete ohmic resistance, and temperature over corrosion time, 0.0 kg/m^3 admixed chloride, outdoor specimens, 51 mm cover depth. *a*) Corrosion rate (Gecor device) vs. time; *b*) corrosion rate (3LP device) vs. times; *c*) concrete ohmic resistance vs. time; and *d*) temperature at depth of reinforcement vs. time.

Weight Loss Corrosion Rate

Three cores 102 mm in diameter were taken through the reinforcing steel from each slab at the time the test specimens cracked. The steel segments were prepared, cleaned, and evaluated according to ASTM G1–90, method C3.5. The mean corrosion rates calculated from the weight loss measurements and the 3LP and Gecor monthly measurements are

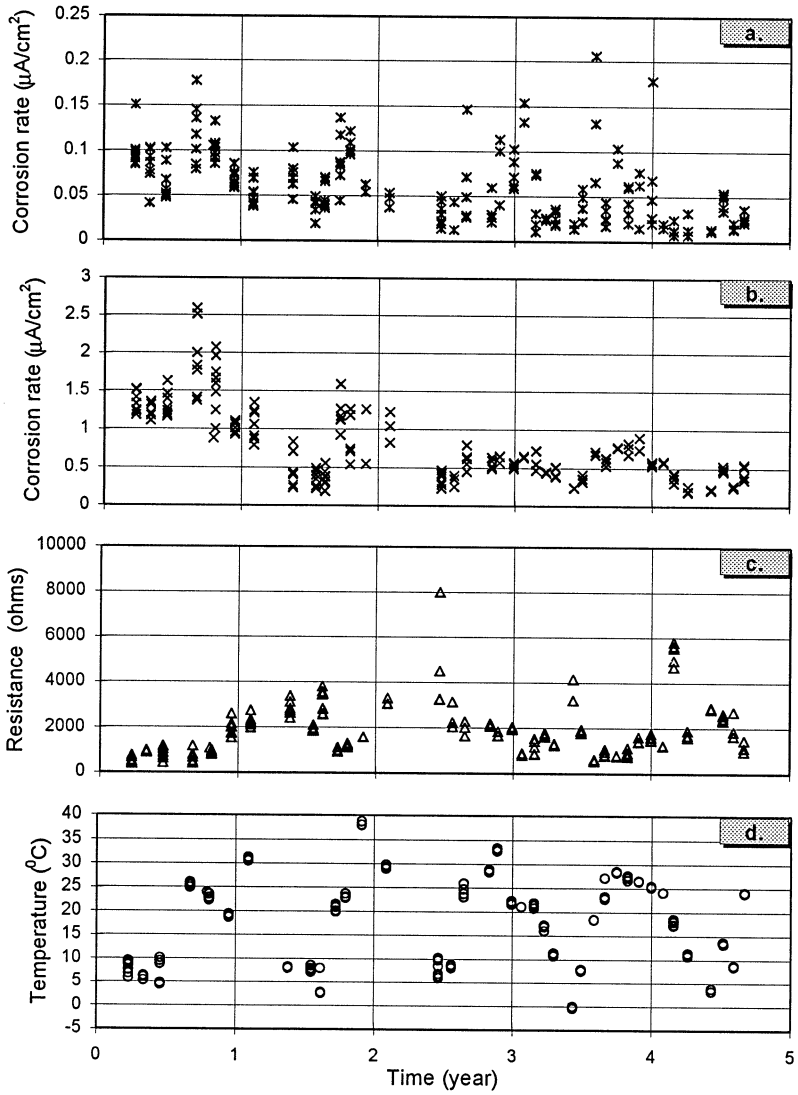

FIG. 3.
Corrosion rate, concrete ohmic resistance, and temperature over corrosion time, 0.71 kg/m^3 admixed chloride, outdoor specimens, 51 mm cover depth. *a*) Corrosion rate (Gecor device) vs. time; *b*) corrosion rate (3LP device) vs. times; *c*) concrete ohmic resistance vs. time; and *d*) temperature at depth of reinforcement vs. time.

presented in Table 4. As shown, there is a significant difference, generally a factor of 15, between the results of the 3LP and Gecor measurements. From Table 4 it appears that the 3LP overestimates the corrosion rate and the Gecor underestimates the corrosion rate. Both devices may polarize only the top portion of the bar but the 3LP polarizes a greater length than the assumed polarized length. These effects for the 3LP device may counter balance each other somewhat, underestimating the corrosion rate by polarizing only the top portion

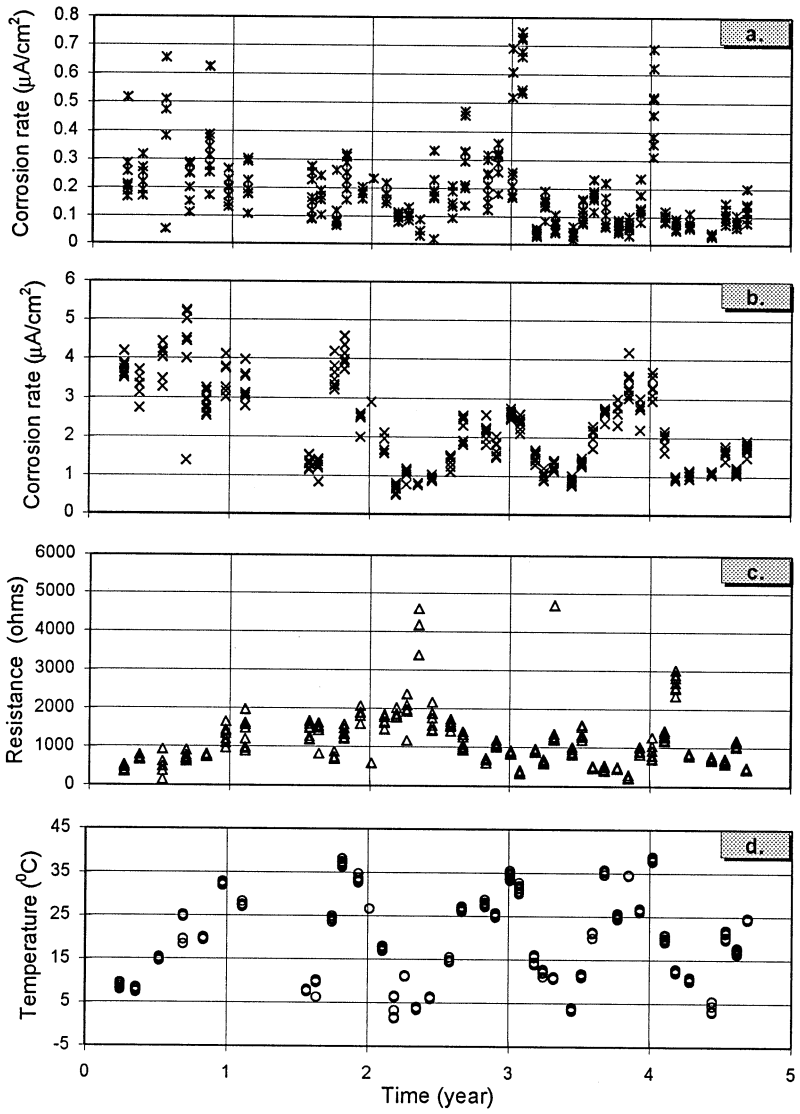

FIG. 4.
Corrosion rate, concrete ohmic resistance, and temperature over corrosion time, 2.85 kg/m^3 admixed chloride, outdoor specimens, 51 mm cover depth. *a*) Corrosion rate (Gecor device) vs. time; *b*) corrosion rate (3LP device) vs. times; *c*) concrete ohmic resistance vs. time; and *d*) temperature at depth of reinforcement vs. time.

of the bar and overestimating by polarizing a longer than assumed bar length. The underestimation of the corrosion rates determined by Gecor may be related to the high interfacial capacitance of steel in concrete with chloride additions (15). Also, the guard ring may concentrate the polarization current over an area smaller than the distance between the midpoints of the guard ring and counter electrode when the corroding area is smaller than this

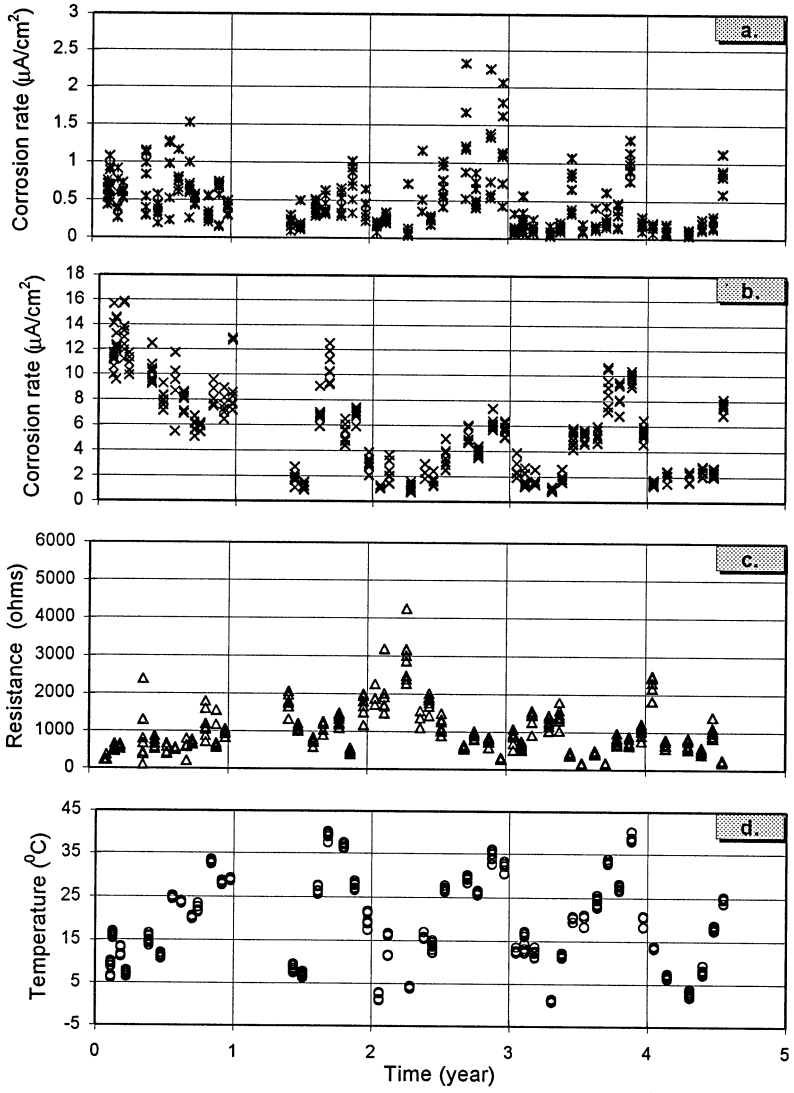

FIG. 5.
Corrosion rate, concrete ohmic resistance, and temperature over corrosion time, 5.69 kg/m^3 admixed chloride, outdoor specimens, 51 mm cover depth. *a*) Corrosion rate (Gecor device) vs. time; *b*) corrosion rate (3LP device) vs. times; *c*) concrete ohmic resistance vs. time; and *d*) temperature at depth of reinforcement vs. time.

distance. For steel bars corroding in concrete, the process is pitting corrosion, and the corroding area is often smaller than the distance between the Gecor guard ring and counter electrode midpoints. Thus, the effect would be for the Gecor to underestimate the corrosion rate.

During this outdoor exposure period, the annual mean temperature in Blacksburg, Virginia, was about 11°C. The device corrosion rate measurements were taken during daytime

TABLE 4
Mean corrosion rates calculated from the 3 measurement methods.

Test series	Exposure period (year)	Mean corrosion rate ($\mu A/ft^2$)		
		Weight loss method	3LP	Gecor
OA2859.6	1.84	2.35	8.49	0.54
OB3859.6	3.67	1.80	4.99	0.42
OE185512.0	0.87	3.77	8.63	0.67
OF18512.0	0.87	3.77	8.85	0.59
Block9.6	2.38	1.81	6.49	0.39

while the temperature at depth of reinforcement varied between 1.7 to 43°C. The mean temperature for measurement times was much higher than that of annual mean temperature. This may cause an overestimation of average corrosion rate. Therefore, the instantaneous corrosion rates from the linear polarization method cannot be directly used for predicting the service life of reinforced concrete structures due to corrosion. It is necessary to develop a model to characterize the corrosion rate, so that the measured corrosion rate from the linear polarization method can be adjusted to an equivalent value based on annual mean temperature and resistance of concrete. The statistical model for characterizing the corrosion rate based on the obtained corrosion data is presented in the following paragraphs.

Modeling

As stated above, the measured corrosion rate varies with changes of temperature, chloride content, resistance of concrete, and corrosion period. Based on previous results (16) a statistical analysis was performed on a set of non-linear models. One of the best models relates the rate of corrosion to concrete temperature, ohmic resistance, chloride content, and exposure time.

The regression results from the corrosion database (2927 measurements from 7 series of chloride contaminated specimens, up to 5 years of outdoor exposure) are as follows:

$$\ln 1.08\, i = 7.89 + 0.7771 \ln 1.69\, \mathrm{Cl} - 3006/T - 0.000116 R_c + 2.24 t^{-0.215} \quad (1)$$

$$s = 0.3312,\ R^2 = 90.1\%$$

where i is the 3LP corrosion rate ($\mu A/cm^2$); Cl is chloride content (kg/m^3); T is temperature at the depth of steel surface (in degree Kelvin); R_c is the ohmic resistance of the cover concrete (ohms); and t is corrosion time (years).

Note that the values of chloride content used for developing this model were obtained from the acid soluble test method (ASTM C1152). However, only free chloride ions influence the corrosion processes. Thus, the following presents the regression equation for water soluble chlorides:

$$\ln 1.08\, i = 8.37 + 0.618 \ln 1.69\, \mathrm{Cl} - 3034/T - 0.000105 R_c = 2.32 t^{-0.215} \quad (2)$$

$$s = 0.3257,\ R^2 = 90.4\%$$

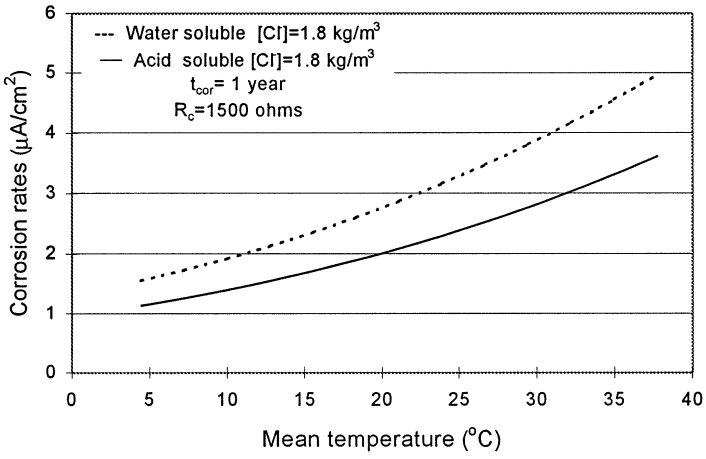

FIG. 6.
Effects of temperature at depth of reinforcement on the corrosion rate.

where the water soluble chloride contents (ASTM C1218) are used in the regression equation.

No correlation was found for the measured corrosion rates obtained from the Gecor device. This is most likely due to the high variations in the measured corrosion rates within the test corrosion cells (16).

Model Interpretations

The effects of significant variables such as temperature, chloride content, corrosion time, and resistance of concrete, which influence the corrosion rate, can be shown from Eqs. 1 and 2, and will be briefly discussed in the following paragraphs.

Temperature

Temperature has a significant effect on the corrosion rate of steel in concrete, as with other chemical and electrochemical reactions. The developed regression model contains a similar temperature relationship to that developed by Clear (17):

$$i_1 = i_2 e^{2283\left(\frac{1}{T2} - \frac{1}{T1}\right)}$$

where i_1 is the corrosion current density at temperature T_1; i_2 is the corrosion current density at temperature T_2; T_1 is the temperature of the concrete at measurement (in degrees K); and T_2 is the temperature that one desires to know the corrosion current density (in degrees K).

In general, corrosion rates increase as the temperature increases. Figure 6 presents the influence of temperature on corrosion rate with the other model parameters held constant.

Because changes of temperature in concrete will also result in changes of other parameters such as resistance of concrete and oxygen diffusion, the overall effect of temperature on corrosion rate in concrete is very complex and controlled by interactions among other factors.

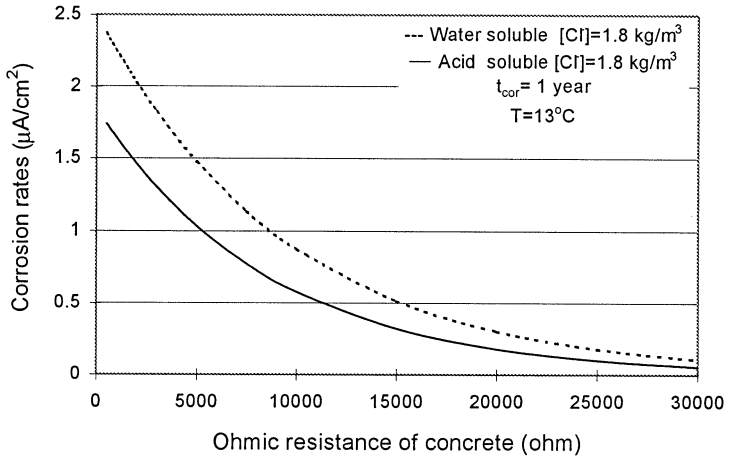

FIG. 7.
Effects of ohmic resistance of cover concrete on the corrosion rate.

In case of a dry environment, the corrosion rate can be relatively small even at a high temperature due to a high resistance of concrete.

Concrete Ohmic Resistance

The degree of saturation of concrete also has a major effect on the corrosion processes; it influences the diffusion of oxygen and the ionic resistance of the concrete. The ohmic resistance of concrete may change significantly from more than 10^4 ohms in a dry environment to about several hundred ohms when concrete is saturated. In fully saturated concrete or dry concrete, the corrosion rate is very low. As is known, corrosion of steel in concrete requires a sufficient supply of oxygen for the cathodic reaction to take place, as well as moisture to act as an electrolyte of low resistance. Usually, the oxygen availability at the steel surface exceeds the amount needed for corrosion for normal outdoor concrete exposures (18). Therefore, corrosion rate of steel in concrete increases as concrete resistance decreases for normal outdoor exposure conditions. The regression model also shows a similar relationship between corrosion rate and ohmic resistance of the concrete. Figure 7 illustrates the influence of degree of saturation on corrosion rate, which varies the ohmic resistance of the concrete.

Only in the case of reinforced concrete structures totally immersed in water is the corrosion rate controlled by the oxygen supply and corrosion takes place very slowly, although the ohmic resistance is very low. Therefore, the model cannot be used for the cases where the corrosion rate is primary controlled by the cathodic reaction.

Chloride Content

The regression results show that the corrosion rate increases as the amount of chloride content increases in concrete, which indicates that corrosion rate will be higher at high levels of chloride contamination. This is the result of an increase in conductivity of concrete as the chloride ions increase, and chloride ions can also complex with ferrous ions to form a water

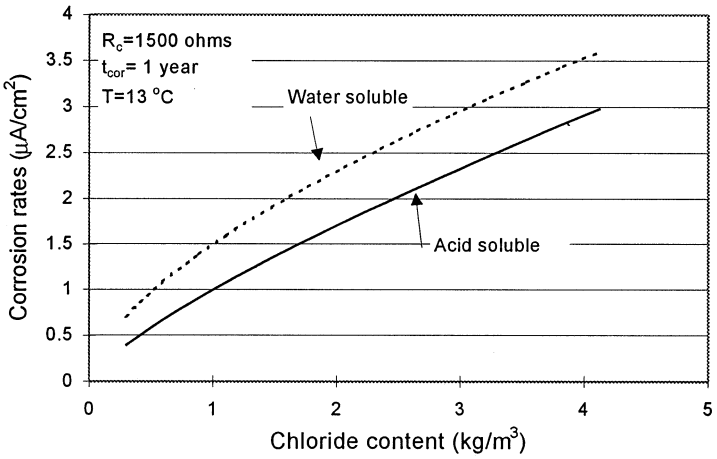

FIG. 8.
Effects of chloride content at depth of reinforcement on the corrosion rate.

soluble product that can also accelerate the corrosion processes. Figure 8 illustrates the effect of chloride content on corrosion rate.

Corrosion Time

Corrosion time has a significant effect on the corrosion rate during early stages after corrosion initiation (see Fig. 9). The corrosion rate decreases rapidly at the early stage (first year after initiation) and then tends to reach a near-constant value. This is due to a reduction in the anode and cathode area ratio, and also results from the formation of the rust products

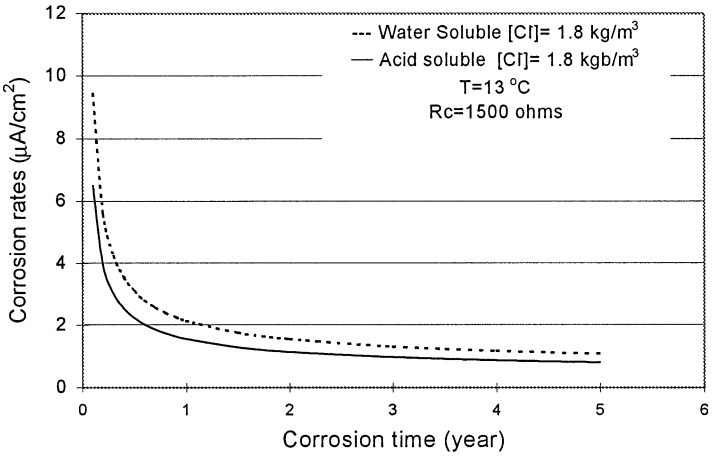

FIG. 9.
Effects of corrosion time on the corrosion rate.

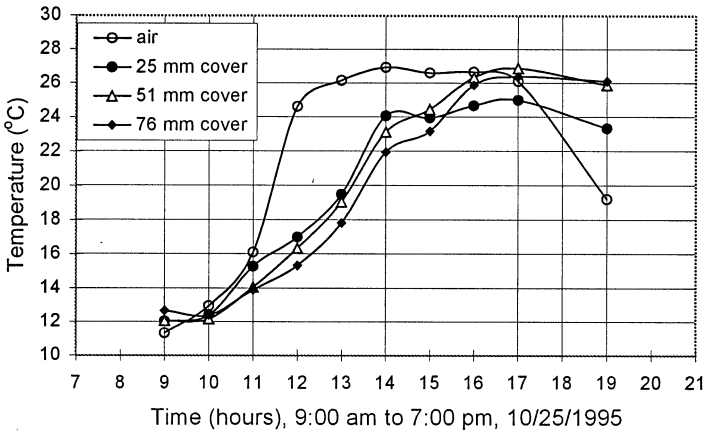

FIG. 10.
Changes of temperatures at different cover depths during a daytime.

on the steel surface, which slows down the diffusion of the iron ions away from the steel surface.

Cover Depth

In the model, the corrosion rate appears not to be affected by cover depth. However, because there is a slight difference in temperature and moisture at different cover depths, these parameters may affect the corrosion rate. The experimental results showed that the corrosion rate at 51 mm cover depth was about 5% higher than that of 76 mm cover depth because there was about 1 to 2°F difference in the mean temperature between two cover depths. Figure 10 presents the change in temperature at different cover depths due to changes of air temperature during a particular day.

Applications

The annual mean temperature is about 11°C in Blacksburg, Virginia. Using Eq. 1, the adjusted corrosion rate can be obtained. The results are summarized in Table 5.

As seen from the above table, the 3LP model adjusted corrosion rates are about 1.5–1.6

TABLE 5
Adjusted corrosion rates and measured corrosion rates.

Series	Corrosion time (yrs)	W_{loss} ($\mu A/cm^2$)	3LP ($\mu A/cm^2$)	Adjusted ($\mu A/cm^2$)	Adj/W_{loss} ($\mu A/cm^2$)
OA2859.6	1.84	2.35	8.49	3.58	1.52
OB3859.6	3.67	1.80	4.99	2.79	1.55
OE(F)18512.0	0.87	3.77	8.85	5.96	1.58
Block9.6	2.38	1.80	6.49	3.01	1.67

times higher than the weight loss measurements. The overestimated corrosion rate is related to polarization area for the 3LP device being larger than the nominal polarization area used in the corrosion current density calculation. Therefore, the equivalent corrosion rate may be taken as the model adjusted corrosion rate divided by a factor of 1.55.

Because the model was developed from the admixed chloride concrete, some adjustment is needed in order to use this model to estimate the corrosion rate for field concrete structures where chloride ions diffuse into the concrete. The difference in chloride concentration in concrete pore solution between admixed chloride concrete and field concrete needs to be further investigated, but may be related to the difference in acid soluble and water soluble chloride models presented in this paper.

As shown in Eqs. 1 and 2, the dynamic rate of corrosion of steel in chloride-contaminated concrete is a function of the concrete chloride content at the bar depth, the concrete temperature at the bar depth, the electrical resistance of the cover concrete, and time after corrosion initiation. The average annual corrosion rate maybe estimated from Eq. 2. As shown in Figures 2 through 5, the resistance of the cover concrete generally varies between 500 and 2500 ohms; thus, it is reasonable to assume an average annual concrete resistance of 1500 ohms for a concrete with a water to cement ratio of about 0.45 in an environment similar to Blacksburg, Virginia. The average annual temperature may be determined from local weather data or other sources, and the time after corrosion initiation may be assumed to be 1 to 3 years for measured water soluble chloride contents greater than 0.5 kg/m^3 (see Fig. 9). Thus, the average annual corrosion rates may be estimated from the measured water soluble chloride contents.

Conclusions

1. The model proposed here based on the experimental corrosion database shows that the corrosion rate is a function of the temperature, ohmic resistance of the cover concrete, chloride content, and corrosion time.
2. The corrosion rate increases with an increase of temperature and amount of chloride ions, and decreases as the ohmic resistance of concrete increases. The corrosion rate decreases rapidly at early stage after corrosion initiation, and then it tends to reach a certain value after about 1 year for constant chloride contents.
3. The corrosion of steel in concrete is a dynamic process; the measured corrosion rate from current devices at one time should be adjusted to an equivalent value to predict service life corresponding with the service exposure conditions such as temperature, moisture, and chloride content.
4. The model-predicted corrosion rates are in good agreement with the results from the weight loss method in accordance with ASTM G1–90, Method C3.5.

References

1. C.L. Page, Instit. Corr. Sci. Tech. Bul. 77 (1979).
2. D.A. Havsmann, Mater. Prot. B, 19 (1967).
3. K.K. Sagoe-Grentsil, Mag. Concr. Res. 41, 205 (1989).
4. K. Tuuti, Corrosion of Steel in Concrete, p. 104, Swedish Coment and Concrete Research Institute, Stochkolm, 1982.
5. P.D. Cady and R.E. Weyers, Cem. Concr. Agg. 2, 81 (1983).

6. Z.P. Bazant, ASCE, J. Str. Div., 105, ST6, 1115 (1979).
7. S. Feliu, J.A. Gonzalez, C. Andrade, and V. Feliu, Corr. 44, 761 (1988).
8. F. Carassiti, E. Proverbio, and T. Valente, Proceedings of 4th International Symposium, Espoo, Finland, p. 647, 1991.
9. P. Schiessel and M. Raupach, Corr. Reinf. Concr. SCI, London, 49 (1990).
10. C. Alonso, C. Andrade, and J.A. Gonzalez, Cem. Concr. Res. 23, 1130 (1993).
11. W. Lopez and J.A. Gonzalez, Cem. Concr. Res. 23, 368 (1993).
12. W. Lopez, J.A. Gonzalez, and C. Andrade, Cem. Concr. Res. 23, 1130 (1993).
13. K.C. Clear, Trans. Res. Rec. 1211, 28 (1992).
14. J.P. Broomfield, J. Rodriguez, L.M. Ortego, and A.M. Garcia, ACI Convention, Minneapolis, Minnesota, 1993.
15. K. Videm, R. Myral, and A S. Rescon, Corr. 96, 169 (1996).
16. Y. Liu and R.E. Weyers, Corr. Reinf. Concr. Const. SCI, London, 88 (1996).
17. Y.P. Virmani and K.C. Clear, FHWA/RD-83/012, 5 (1983).
18. C. Andrade, C. Alonso, I. Rz-Maribona, and M. Garcia, ACT, Paul Kieger Conference, San Diego, 1989.